

SMALL SCALE PARALLEL FLOW CONTACT EROSION TEST BETWEEN SAND AND SILTY CLAY LAYERS

*Pradeep Pokhrel¹, Jiro Kuwano¹

¹Department of Civil and Environmental Engineering, Saitama University, Japan

*Corresponding Author, Received: 24 July 2020, Revised: 13 Aug. 2020, Accepted: 01 Sept. 2020

ABSTRACT: Internal erosion is one of the major causes of the failure of hydraulic structures, road pavement, and the naturally deposited ground as well. Except suffusion and piping, contact erosion is also a type of internal erosion that can mostly occur at the foundation of embankment dams and dikes, in the road pavement and the alluvial fan deposited valley. This phenomenon occurs when the seepage flow exists at the interface of fine and coarse soil layers where fine particles are detached and transported through the voids of the coarse soil layer. Between 2013-2017 numerous sinkholes have been observed in Armala area of Pokhara valley in central Nepal. The locations of the sinkholes mainly observed at paddy fields in the alluvial fan deposit. The sinkhole affected area was investigated twice in the year 2015, 2016, and 2017. Based on the subsurface ground condition and the location of the hidden cavity, it assumed that an internal contact erosion occurred, and this phenomenon leads to the formation of subsurface hidden cavity and collapse sinkholes in the Armala area. Mechanics of contact erosion was studied in the laboratory by performing a series of small-scale parallel flow contact erosion test. The physical model of the experiment was prepared with the soil having a similar grain size and physical properties to the onsite granulometry. A cavity was observed at the interface when the fine soil (DL clay) is overlying the coarse sand. Also, the amount of discharged soil decreases with the increase of overburden pressure.

Keywords: Sinkhole, Borehole, Contact erosion, Flow velocity, Piping

1. INTRODUCTION

Most of the hydraulic structures are failed caused by internal erosion due to seepage flow. In recent years, subsurface cavities or collapsed sinkholes in the road pavement and naturally deposited ground are widely observed worldwide. Various types of internal erosion can take place in the subsurface of the ground. Like suffusion and piping, contact erosion is also a type of internal erosion that can mostly occur at the foundation of embankment dams and dikes, in the road pavement and the alluvial fan deposition valley. Contact erosion occurs when the seepage flow exists at the interface of fine and coarse soil layers where fine particles are detached and transported through the voids of the coarse soil layer. Various research has been conducted on contact erosion in the context of dikes [1], embankment dams [2,3,4], and road pavement [5]. Previous authors [1,2,3,4] conducted a parallel flow contact erosion test simulating the internal contact erosion that most frequently encountered in the hydraulic structures. A perpendicular flow contact erosion test was performed to simulate the internal contact erosion below the pavement layers due to the fluctuation of the water table [5]. For the significant occurrence of parallel flow internal contact erosion, two conditions should be fulfilled [1,2,3,4]. The first one is the geometrical condition where the size of

the voids of coarse soil should be large enough than the grain size of the fine soil. So that all the fine particles can pass through the voids of coarse soil. The second is the hydraulic condition, where the seepage velocity is high enough to scour and transport the fine particles through the void of the coarse soil. In the past, the research [1,2,3,4] mainly focuses on the artificial hydraulic structure, and they used the gravel and the mixture of sand and gravel as coarse material considering the suitable material for the filter layer of hydraulic structures.

This study focuses on the internal contact erosion to understand the phenomenon that leads to sinkhole formation using the soil material having similar physical and geometrical properties of the onsite soil. The maximum grain size of the coarse soil used in this study is significantly smaller than the coarse soil used in previous research. The effect of overburden pressure on the erosion rate was studied.

1.1 Background of the Research

From November 2013 to 2017, numerous (more than 200) sinkholes have been observed in the Armala area of Pokhara valley in central Nepal. The locations of the sinkholes were observed mostly at paddy fields in the alluvial fan deposit. An example of a sinkhole in the Armala area is shown in Fig.1. The subsurface materials deposited in the sinkhole

affected area are silty clay, sand, and gravel. The sinkhole affected area was investigated twice in the year 2015, 2016, and 2017. The results obtained from the investigation were reported in [6,7,8,9]. During the investigation, a borehole logging with a standard penetration test (SPT) was conducted at one point near the observed sinkhole. A thick white silty clay layer was found at a depth of 4 m to 20 m from the ground level [7, 8, 9]. In addition, a hidden cavity 2.5 m thick was discovered at a depth of 7.5 m to 10 m from the ground level.



Fig.1 A sinkhole in the Armala area, Nepal.

In order to study the soil strata parallel to the sinkhole cavity discovered from the borehole survey, some scarp located on the right bank of the nearby river (Kali Khola) was also observed. It identified from these scarps that a 0.05 m thick sand seam layer lies in between the silty clay layers at a depth of 9 m from the ground surface, which is the same level as the sinkhole cavity discovered from the borehole investigation. Fig.2 shows the outcrop just after the shaping (left), groundwater discharged after 5 minutes (center), and eroded silty clay in the form of slurry after 11 minutes (right). The orientation of the soil strata at the outcrops is illustrated in a schematic diagram in Fig.3. At the outcrop, discharged groundwater was observed at the interface of sand and silty clay layers after 5 minutes of shaping. It is possibly due to the

presence of a high permeable sand layer between the silty clay layers. The discharge of groundwater took place at both the upper and lower interface of a sand layer, which is attached to the silty clay layers. In addition, more amount of discharged water was observed at the upper interface of a sand layer, i.e., silty clay layer overlying a sand layer at the outcrop. However, internal erosion was observed at both the side of a sand layer, and therefore, the presence of a sand layer could be one of the factors to trigger internal contact erosion on the site. Internal erosion was not taking place at that location if there was only the presence of silty clay in the subsurface of Armala.

The primary source of groundwater flow in the sinkhole affected area is seepage from the hillside to the mainstream. The path of seepage flow from the source to the exit shows that the groundwater flows parallel to the interface of soil layers. All this evidence shows that the presence of a sand seam within silty clay layers could be one of the factors to trigger parallel flow internal contact erosion and hidden cavity formation in the Armala area. Therefore, a series of small scale parallel flow contact erosion tests were conducted in the laboratory to observe the contact erosion and its phenomenon to lead the cavity formation. The physical model of the experiment was prepared with the soil having a similar grain size and physical properties to the onsite granulometry. The maximum grain size of the coarse sand used in this study is 2.3 mm, which is significantly smaller than the coarse soil used in previous research [1,2,3,4].

2. EXPERIMENTAL SETUP

The schematic diagram of the parallel flow contact erosion test apparatus is shown in Fig.4. It consists of two water tanks, inlet, and outlet connected to a U-shape acrylic box containing a fine and coarse soil combination. The overall inner dimension of the U-shape acrylic box is 30 cm long, 12 cm wide and 15 cm high. Base plate, porous plate, DL clay layer, sand layer, porous plate, and the loading plate is placed in sequence from the bottom

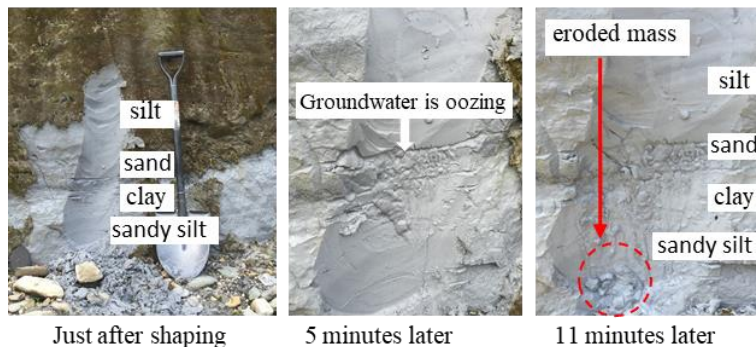


Fig.2 Groundwater oozing from the sand layer.

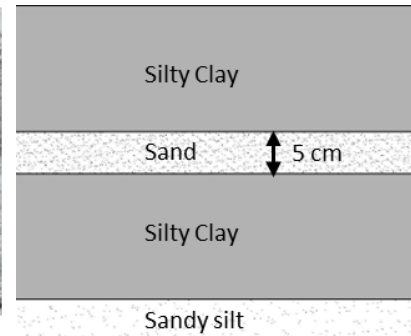


Fig.3 Illustration of soil strata at the outcrops.

to the top. In each test, a 10 cm thick DL clay layer and 1 cm thick sand layer were used for both configurations, i.e., fine soil overlying the coarse soil and coarse soil overlying the fine soil. An acrylic plate of 1 cm × 12 cm opening was placed between the soil chamber and inlet-outlet boxes so that the openings of the soil specimen box coincide with the cross-section of the coarse sand layer. Steel mesh of sieve No. 150 was placed at the opening of the plate. So that only DL clay can pass through the mesh. When the valve is open, water flows through the coarse sand layer and parallel to the fine soil surface. A belloram cylinder is connected to the loading rod through a load cell to apply the overburden pressure to the soil sample to simulate the overburden pressure on the site.

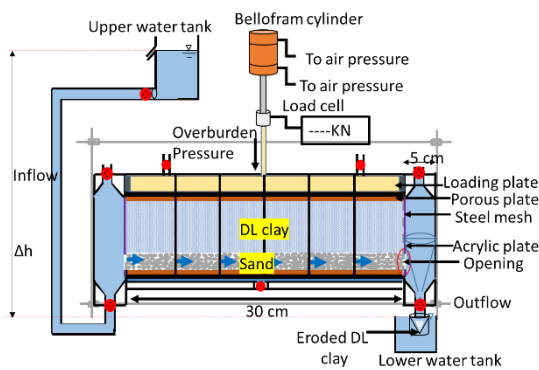


Fig.4 Schematic diagram of parallel flow contact erosion test apparatus.

A series of experiments were performed with the stepwise increase in water head difference at the time interval of 30 minutes under constant overburden pressure. With the increase of water head difference, the flow velocity increases as well. Flow velocity, V (cm/s) is calculated by using the formula $V = Q/A_c$ where Q (cm^3/s) is the discharged water measured, which depends on coarse sand permeability, and A_c (cm^2) is the cross-section area of the coarse sand which is same as the cross-section of the opening.

The turbidity of the discharged water was measured in every 5 minutes of each interval to find the concentration of DL clay in the discharged water.

3. TESTED SOILS

The white silty clay located in the hidden cavity is a non-plastic silty clay composed of 79% silt, 16% clay, and 5% sand. The grain size distribution of this white silty clay was analyzed by conducting a hydrometer test and sieve analysis method. The D_{10} , D_{30} and D_{60} grain size of this silty clay soil are 0.0014 mm, 0.005 mm, and 0.023 mm, respectively. Test material used in this study comprised of DL clay, which is the commercial name of the soil and

silica sand No.3 and silica sand No.5. DL clay is non-plastic silt composed of 90% silt and 10% clay, which shows the similar properties and grain size of silty clay found in the Armala area. In this study, DL clay was considered as fine soil, whereas silica sand No. 3 and silica sand No. 5 were considered as coarse material. Figure 5 shows the gradation curve of the tested soils. The median grain size of silica sand No. 3, silica sand No. 5, and DL clay is 1.6 mm, 0.6 mm, and 0.028 mm, respectively. The maximum grain size of the coarse sand is 2.3 mm, which is significantly finer than the coarse soils used by the previous researchers for the contact erosion test. The geometrical and physical properties of the tested soils are given in Table 1.

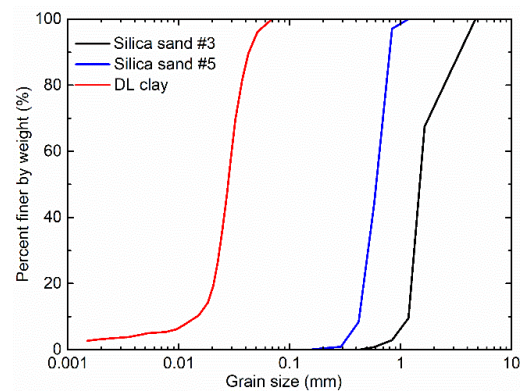


Fig.5 Particle size distribution of tested soils.

Table 1 Geometrical and physical properties of soils.

Properties	Unit	DL clay	Silica sand#3	Silica sand#5
ρ_s	g/cm ³	2.654	2.56	2.56
ρ_{dmax}	g/cm ³	1.538	1.462	1.543
ρ_d	g/cm ³	1.384	1.388	1.383
D_{15}	mm	-	1.3	0.45
D_{50}	mm	0.0280	1.6	0.6
D_{85}	mm	0.0395	-	-
C_u	-	1.935	1.417	1.553
C_c	-	1.168	0.961	0.927
K_s	m/s	6×10^{-7}	5×10^{-4}	1×10^{-4}

Where, ρ_s – density of the particle, ρ_{dmax} – maximum dry density, ρ_d – dry density, D_{15} – 15 % percentile of soil grain size, D_{50} – median grain size of soil, D_{85} – 85 % percentile of soil grain size, C_u – coefficient of uniformity, C_c – coefficient of curvature, K_s – coefficient of permeability

In 1984, Sherard [10, 11] proposed the D_{15}/d_{85} ratio as a filtering criterion, where D_{15} (mm) is the 15% percentile of the coarse soil grain size, and d_{85} (mm) is the 85% percentile of the fine soil grain size. Based on the experiments, they found that filtering

criteria are $D_{15}/d_{85} \leq 4$ and $D_{15}/d_{85} \leq 9$, depending on the fine soil. The tested soils, in this study, do not validate this criterion. It means the void size of the sand used in the test has large enough to pass the totally or partially the grain of DL clay.

The fine soil was prepared at optimum water content and compacted five successive layers of 2 cm thick in the soil chamber to achieve the 90% of the maximum density by static compaction method. The corresponding dry density of fine soil at 90% degree of compaction is 1.384 g/cm^3 . Coarse sand was placed manually at the relative density of 50% and its corresponding dry density of silica sand No. 3 and silica sand No. 5 are 1.388 g/cm^3 and 1.383 g/cm^3 , respectively. The permeability of the fine soil $6.68 \times 10^{-7} \text{ m/s}$ is significantly smaller than the permeability of coarse soil $1.26 \times 10^{-4} \text{ m/s}$. So that water will flow only through the coarse soil layer.

4. EXPERIMENTAL PROGRAM

In this study, six parallel flow contact erosion tests were performed, considering the configuration of fine and coarse soil combination, types of coarse material, and the applied overburden pressures. Two configurations, coarse sand overlaying the DL clay and DL clay overlaying the coarse sand, were used in the tests. The collapsed sinkholes found in the Armala area were usually shallow in the depth of about 1 to 5.5 m. Considering the depth of the cavity and sinkhole discovered at the site, 40 kPa and 70 kPa overburden pressure were applied in the tests. Test conditions are summarized in Table 2.

Table 2 Test conditions

Test No.	Soil configuration	Overburden pressure (kPa)
1	*SS #3 / DL clay	40
2	SS #3 / DL clay	70
3	DL clay / SS #3	40
4	DL clay / SS #3	70
5	DL clay / SS #5	40
6	DL clay / SS #5	70

*SS-Silica sand

5. EXPERIMENTAL RESULTS

5.1 Observation of Erosion at the interface

When the valve is open, water flows through the coarse sand at the interface of DL clay and sand layers. All the experiments were started with the small flow velocity. At low flow velocity, no erosion at the interface was observed. Also, the measured turbidity value of the discharged water corresponding to the small flow velocity was small.

It means the shear force generated by the water flow was smaller than the stress to cause erosion of the fine particles at the interface. With the increase of flow velocity, continuous erosion was observed at the interface.

In the case of coarse sand overlaying the DL clay, the coarse sand grain collapse was observed even in low erosion rates. Probably, it was due to the non-cohesive behavior of coarse sand. At the time of continuous erosion, both the fine and coarse soil particles at the interface were in an unstable state. Fine particles at the interface were detached and transported through the voids of coarse material due to flow. Simultaneously, the rate of erosion tended to increase, but the unstable coarse particles were not able to transmit the overburden stress. Indeed, the unstable coarse particles collapsed due to gravity, and clogging was observed. So, the amount of eroded soil may have been affected by this clogging effect. Pokhrel [12,13,14] also observed a similar phenomenon when the coarse sand overlaying the fine sand. The observation result shows that the contact erosion phenomenon in this configuration leads to the surface settlement if the coarse material is a non-cohesive and uniformly graded soil. The propagation of erosion with time is shown in Fig.6.

In the case of DL clay overlaying the coarse sand, a cavity was observed at the interface. The arch of the cavity formed by the erosion seemed stable due to the cohesion of DL clay [15]. During the continuous erosion, the fine soil at the interface flowed out with water, where a piping phenomenon was observed. The density of the DL clay decreases at the interface with continuous erosion and resulting in the concentration of flow at the location. With the passage of time, the flow concentrated at the unstable part, and the cavity propagates in the horizontal and vertical directions. The observation result shows that the contact erosion phenomenon in this configuration leads to the formation of a subsurface cavity and finally collapses to form a sinkhole. The propagation of erosion with time when DL clay overlaying the silica sand is shown in Fig.7.

5.2 Concentration of DL Clay in the Discharged Water and Critical Flow Velocity

The concentration of the soil particles in the discharged water is the key factor in analyzing the behavior of erosion with time. The flow velocity having non-zero turbidity is considered as threshold velocity to initiate the contact erosion of fine soil [2,3,4]. The turbidity of the discharged water was measured in every 5 minutes of each interval of 30 minutes. The relationship between the water turbidity and the concentration of DL clay contained in water was obtained from the several

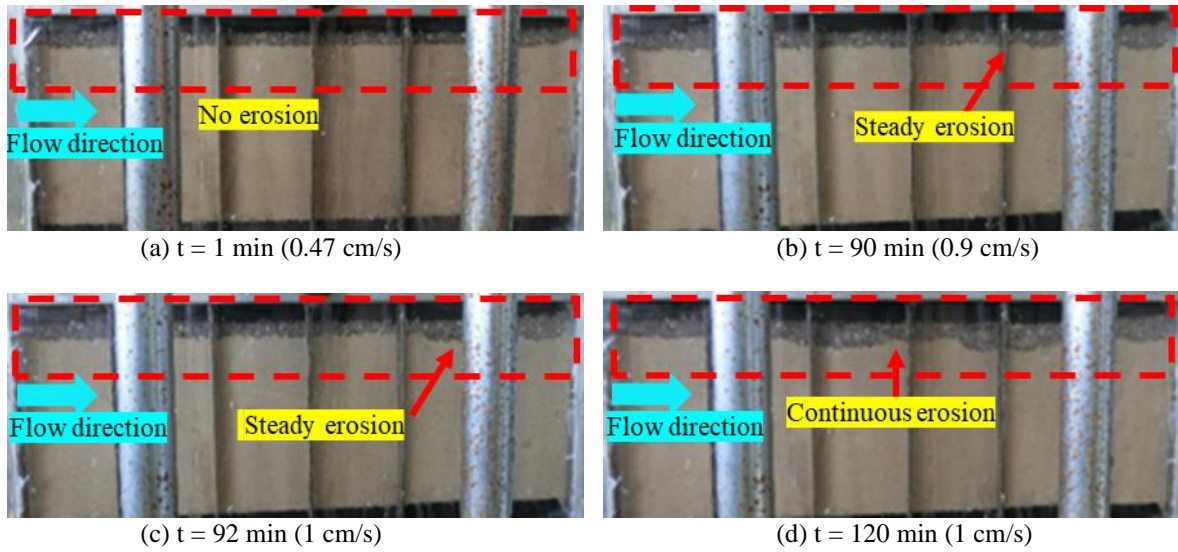


Fig.6 The propagation of erosion with time (Coarse sand overlying the DL clay).

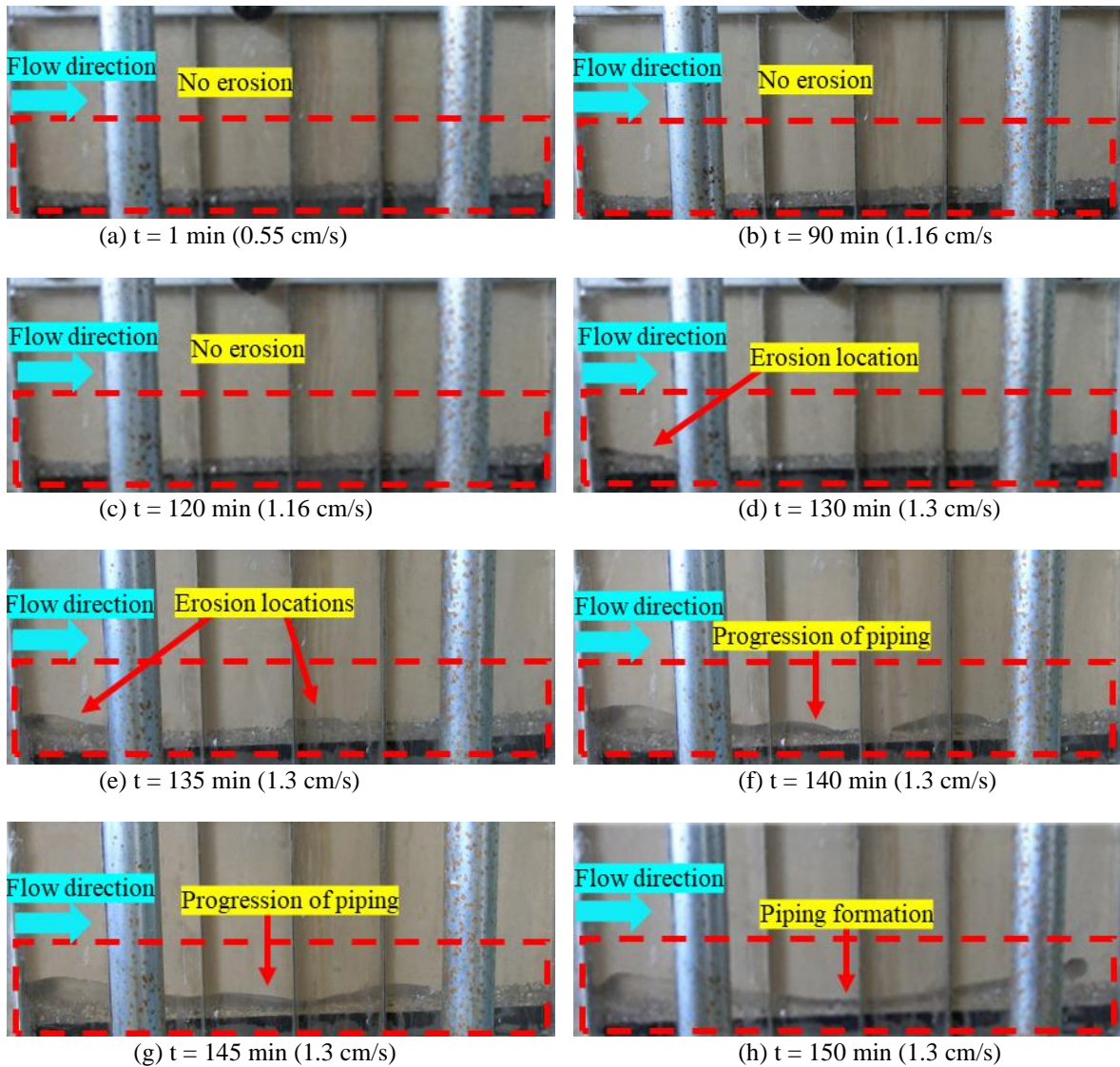


Fig.7 The propagation of erosion with time (DL clay overlying the coarse sand).

measurements of turbidity by sampling from 1 liter of clean water containing various predetermined quantities of soil particles. Figure 8 presents the test result of the relationship of water turbidity with DL clay concentration.

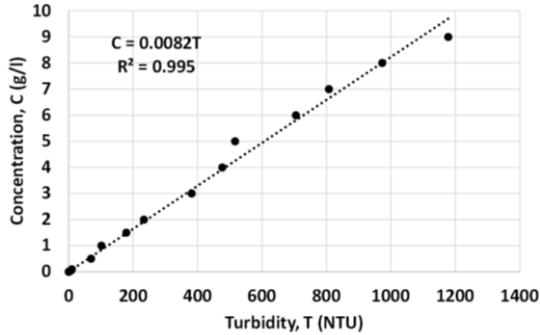


Fig.8 The relationship between water turbidity and DL clay concentration.

The correlation between water turbidity and the concentration of DL clay particles is presented as follows.

$$C \text{ (g/l)} = 0.0082 \times T \text{ (NTU)} \quad (1)$$

where, $C \text{ (g/l)}$ – concentration (gram per liter)
 $T \text{ (NTU)}$ – Turbidity

The eroded fine particles may settle in the discharge pipe, which may affect the turbidity measurement and the erosion rate. To cross-check the validity of turbidity measurement, discharged water containing DL clay particles was also measured through sampling. In this method, the discharged water was collected for 5 seconds every 5 minutes. The weight of all the samples was measured. Then they were placed in an electric oven to measure the dry weight of soil. The result of flow velocity, eroded mass measured through sampling, and turbidity with time at different overburden pressure are shown in Figs.9 and 10.

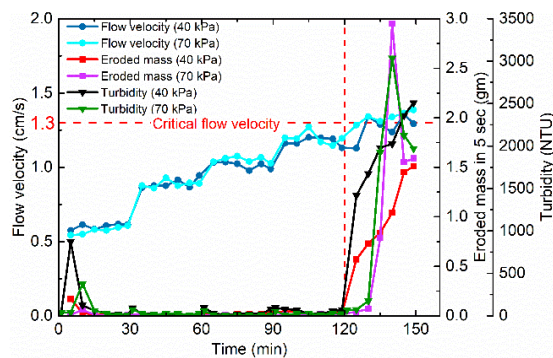


Fig.9 Changes of flow velocity, turbidity, and eroded mass with time (DL clay / silica sand #3).

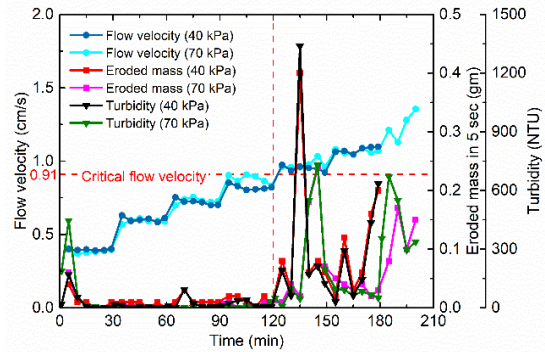


Fig.10 Changes of flow velocity, turbidity, and eroded mass with time (DL clay/silica sand #5).

The concentration of the DL clay in the discharged soil was zero at low flow velocity. The concentration increases significantly with the increase of flow velocity from a certain threshold value. This threshold flow velocity is called the critical flow velocity to initiate the internal contact erosion of DL clay. The turbidity value and the sampling eroded mass show that continuous erosion began after 120 minutes, which corresponds to the flow velocity of 1.3 cm/s in the case of coarse silica sand No. 3 and 0.91 cm/s in the case of the silica sand No.5. The critical flow velocity of specific fine soil depends on the grain size and porosity of the corresponding coarse soil and its porosity [1]. The fluctuation pattern of measured eroded mass and the turbidity of the discharged water are similar. The measured data using a turbidity meter is consistent with the measured mass.

The critical flow velocity obtained from experimental results was compared with the critical flow velocity proposed by Guidoux [2] as Eq. (2).

$$u_{cr} = 0.7n_F \sqrt{\left(\frac{\rho_s - \rho_w}{\rho_w}\right)gd_H \left(1 + \frac{\beta}{d_H^2}\right)} \quad (2)$$

Where, u_{cr} (m/s) - critical flow velocity, n_F - porosity of coarse soil, ρ_s (kg/m³) - density of fine soil grains, ρ_w (kg/m³) - density of water, g (m/s²) - gravity acceleration, d_H (m) - effective diameter of fine soil, β (m²) - adhesive properties of particles.

The critical flow velocity calculated from Eq. (2) using $n_F = 4$ and $\beta = 5.3 \times 10^{-9}m^2$ is 1.8 cm/s. The critical flow velocity obtained from the experimental results of this study is smaller than the critical flow velocity calculated by Eq. (2) proposed by Guidoux [2]. The critical flow velocity obtained from experimental results using silica sand No. 3 as a coarse soil is 1.3 cm/s, whereas using silica sand No. 5 as a coarse soil is 0.91 cm/s. The experimental result shows that the fine soil's (DL clay) critical

flow velocity depends not only on the grain size of fine soil but also on the grain size of coarse soil. The value of the specific fine soil's critical flow velocity decreases with the decrease in the grain size of the coarse soil. The value of the critical flow velocity of fine soil (DL clay), compared to the calculated value of Guidoux [2], decreases by 27.7 % in the case of silica sand No. 3 whereas 49.4% in the case of silica sand No. 5. The coarse soil grain size used in this study is significantly smaller than that of the material used by previous researchers.

5.3 Effect of Overburden Pressure on the Amount of Eroded Mass

The discharged water containing eroded soil mass in each interval of the experiments was collected in a container, and the amount of discharged soil was measured using the turbidity meter. The turbidity of the soil water solution in each container was measured six times, and the average turbidity value was used to calculate the discharged amount of soil in the container. Then the discharged amount of soil in each interval was calculated using the correlation between concentration and water turbidity refer to "Eq. (1)". The cumulative eroded soil mass with flow velocity and time in each experiment is plotted and shown in Fig.11 and 12.

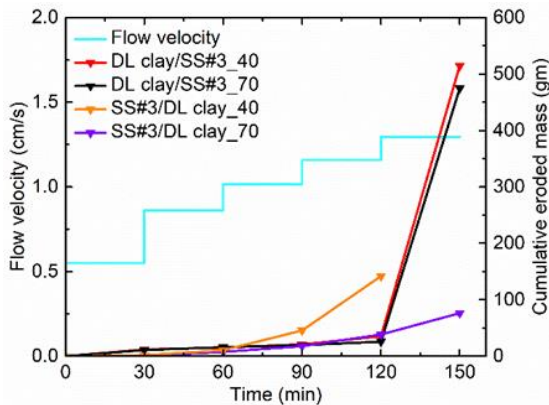


Fig.11 Cumulative eroded mass and flow velocity changes with time (Test cases 1, 2, 3, and 4).

The effect of overburden pressure on the amount of eroded mass or erosion rate was seen in the graph of cumulative eroded mass. In each configuration of soil, the amount of eroded mass of DL clay at 40 kPa overburden pressure is high compared to the 70 kPa overburden pressure, especially in the case sand overlies DL clay.

The coarse soil layer is compressed with the increase in overburden pressure, and this effect is more likely on the small grain size of the soil. The contact surface between fine soil and coarse soil increases with compression. The total volume of

voids in the coarse soil layer decreases. It results in the less amount of the fine particles transported through the voids. The permeability of the coarse soil also decreases with the compression. Therefore, overburden pressure has an inverse effect on the erosion rate.

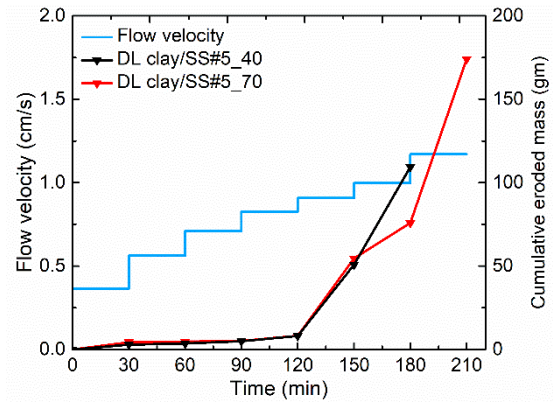


Fig.12 Cumulative eroded mass and flow velocity changes with time (Test cases 5 and 6).

5.4 Possible Mechanism of Internal Erosion in Armala

Internal erosion is the detachment and transportation of fine particles through the voids of coarse material in the subsurface due to seepage forces. The shear force generated by the seepage water should be high enough to scour and erode the subsurface material to initiate internal erosion. The research was initiated after facing the sinkhole problems in the Armala area, Pokhara, Nepal. The groundwater flow from the hillside is a triggering factor to cause internal erosion and sinkhole formation in the Armala area. Pokhrel [6] assumed that the internal erosion occurs between the gravel and surface layer to trigger the sinkhole formation. After the follow-up survey in 2016 and 2017, [7,8,16] confirmed that the erosion occurred within the white silty clay layers.

As mentioned in the background of the research, contact erosion was initiated at the interface of silty clay and sand seam in the Armala area. When the groundwater flowed through the sand seam, the sand and the surficial part of the white silty clay at the interface got saturated. The saturated part of the silty clay lost its stability and was detached and transported through the sand seam. According to the local residents, excavation of aggregates from the riverbed of the mainstream was started from the 1990s for commercial purposes. Due to the excavation of aggregate, the riverbed of the mainstream was lowered with time. As it was the main difference between before and after sinkholes, it was thought to be a possible cause of sinkholes. It increased the hydraulic gradient in the ground and

the subsurface water velocity. Therefore, the hydraulic condition for the internal contact erosion was fulfilled, and then contact erosion causing cavities was accelerated. Experimental results show that the contact erosion is highly accelerated with piping formation when the fine soil overlies the coarse sand. A similar phenomenon was expected in the Armala area. A large amount of subsurface fine materials was eroded, and subsurface cavities were formed. With time, the subsurface cavities increase width and height and finally collapse as a sinkhole. When the riverbed was filled, no more sinkhole was formed, probably because the hydraulic gradient decreased, and the flow velocity in the ground became lower than the critical value.

6. CONCLUSIONS

A series of contact erosion tests were conducted, and the possible mechanism of internal erosion in the Armala area was studied. The following conclusions were drawn from the study.

- 1) Contact erosion is insignificant at low flow velocity but significant when the flow velocity is greater than a certain threshold velocity called a critical flow velocity.
- 2) A cavity was observed at the interface when the DL clay overlies the sand layer. The piping phenomenon was observed in this configuration, which leads to a large amount of erosion rate.
- 3) The observation result shows that the contact erosion phenomenon leads to the surface settlement if the coarse material is non-cohesive and uniformly graded under the soil configuration of coarse material overlying the fine soil condition. But erosion phenomenon leads to the formation of a subsurface cavity under the soil configuration of fine soil overlying the coarse material condition.
- 4) The measured amount of eroded mass under different pressures of 40 kPa and 70 kPa shows that overburden pressure has an inverse effect on erosion rate. Also, the amount of eroded mass of fine soil is high when the fine soil is overlying the coarse soil.
- 5) The test results indicated that the fine soil overlying coarse soil scenario clearly shows the internal erosion that ultimately leads to piping. This situation reflects the Armala site condition that undergoes sinkholes.

REFERENCES

- [1] Bezuijen A., Klein Breteler M., and Bakker K.J., Design criteria for placed block revetments and granular filters. Conference proceedings, in Proc. 2nd Int. Conf. on Coastal and Port Engineering in Developing Countries, Beijing, China, 1987, pp. 1-15.
- [2] Guidoux C., Faure Y.-H., Beguin R., and Ho C.-C., Contact erosion at the interface between granular coarse soil and various base-soils under tangential flow condition. *J. Geotech. Geoenviron. Eng.*, Vol. 136, Issue 5, 2010, pp. 741-750.
- [3] Beguin R., Faure Y.-H. Guidoux C., and Philippe P., Hydraulic Erosion along the Interface of Different Soil Layers. Conference proceedings, in Proc. 5th Int. Conf. on Scour and Erosion, San Francisco, USA, 2010, pp. 387-396.
- [4] Philippe P., Beguin R., and Faure Y. H. Contact erosion, In *Erosion in Geomechanics Applied to Dams and Levees*, Wiley/ISTE, 2013, pp. 101-192.
- [5] Jegatheesan P., Sothilingam P., Arulrajah A., Disfani M. M., and Rajeev P., Laboratory Model Test on Contact Erosion of Dispersive Soil Beneath Pavement Layers. *Geotechnical Testing Journal*, Vol. 38, No. 6, 2015, pp. 1-9.
- [6] Pokhrel R. M., Kiyota T., Kuwano R., Chiaro G., Katagiri T., and Arai I., Preliminary Field Assessment of sinkhole damage in Pokhara, Nepal. *International Journal of Geoengineering Case histories*, Vol. 3, No. 2, 2015, pp. 113-125.
- [7] Kuwano R., Kiyota T., Pokhrel R. M., Katagiri T., Ikeda T., Yagiura Y., Yoshikawa T., and Kuwano J., Investigation into the multiple recent sinkholes in Pokhara, Nepal. Conference proceedings, in Proc. 8th Int. Conf. on Scour and Erosion, UK, 2016, pp. 1117-1122.
- [8] Yagiura Y., Takemasa M., Yoshikawa T., Kiyota T., Katagiri T., Ikeda T., and Pokhrel R. M., Follow-up survey of sinkhole damage in Pokhara, Nepal – Riverbed Lowering and Subsequent Groundwater Lowering Causing Numerous Sinkholes in Pokhara, Nepal Since 2013-. Conference proceedings, in Proc. 7th Japan-Taiwan Workshop on Geotechnical Hazard from Large Earthquake and Heavy Rainfall, Taiwan, 2017.
- [9] Pokhrel P., Kuwano J., Kiyota T., Kuwano R., Ikeda T., Yagiura Y., Pokhrel R. M., Site investigation results of sinkhole affected area in Armala, Pokhara, Nepal. Conference proceedings, in Proc. 14th Regional Conf. of Japan Geotechnical Society Kanto Branch, Japan, 2017, pp. 265-268.
- [10] Sherard J. L., Dunnigan L. P., and Talbot J. R., Basic properties of sand and gravel filters. *J. Geotech. Eng.*, Vol. 110, No. 6, 1984a, pp. 684-700.
- [11] Sherard J. L., Dunnigan L. P., and Talbot J. R., Filters for silt and clays. *J. Geotech. Eng.*, Vol. 110, No. 6, 1984b, pp. 701-718.
- [12] Pokhrel P., Kuwano J., Effect of flow velocity on contact erosion between fine and coarse sand

- layer. Conference proceedings, in Proc. 53rd Japan National Conf. on Geotechnical Engineering, Japan, 2017, pp. 977-978.
- [13] Pokhrel P., Kuwano J., Experimental study of contact erosion between fine and coarse sand layer. Conference proceedings, in Proc. 7th Korea-Japan Geotechnical workshop, Korea, 2018, pp. 21-23.
- [14] Pokhrel P., Kuwano J., Laboratory model test on contact erosion between fine and coarse sand layer. Conference proceedings, in Proc. 54th Japan National Conf. on Geotechnical Engineering, Japan, 2019, pp. 889-890.
- [15] Pokhrel P., Kuwano J., Parallel flow contact erosion test between coarse sand and silty clay layer. Conference proceedings, in Proc. 10th Int. Conf. on Scour and Erosion, USA, 2020 (In press).
- [16] Bhandari B., Bhusal J., Pokhrel R. M., Paudel L. P., Morphology and depositional setting of the sinkhole affected Armala area, Kaski District, western-central Nepal. Journal of Nepal Geological Society, vol. 59, 2019, pp. 59-64.

Copyright © Int. J. of GEOMATE. All rights reserved, including the making of copies unless permission is obtained from the copyright proprietors.
